Estimation of Inferior Vena Cava Size from Ultrasound Imaging in X-Plane

Terms of use:

Publisher copyright

(Article begins on next page)

02 September 2025

Technical Note

Estimation of Inferior Vena Cava Size from Ultrasound Imaging in X-Plane

Piero Policastro and Luca Mesin *

Mathematical Biology and Physiology, Department Electronics and Telecommunications, Politecnico di Torino, 10129 Turin, Italy; piero.policastro@polito.it
* Correspondence: luca.mesin@polito.it; Tel.: +39-0110904085

Abstract: Ultrasound (US) scans of the inferior vena cava (IVC) provide useful information on the volume status of a patient. However, their investigation is user-dependent and prone to measurement errors. An important technical problem is the objective difficulty in studying a very compliant blood vessel like IVC, which makes large respirophasic movements and shows a complicated three-dimensional geometry. Using bi-dimensional (2D) B-mode views either in a long or short axis has improved the characterization of IVC dynamics compared to measurements along a single direction (M-mode). However, specific movements of the IVC can also challenge the information provided by these 2D sections. Thus, these two orthogonal views, provided by an US system in the X-plane, are integrated here using an innovative method. It is tested on simulated videos of the IVC by performing complicated movements, which are compensated by the new method, overcoming the biased measurements provided by 2D scans. The method is then applied on example experimental data.

Keywords: inferior vena cava; ultrasound; tracking; volume estimation; simulation

1. Introduction

Veins, due to their unique structure, exhibit movements and size changes over time, primarily influenced by transmural pressure, defined as the difference between internal and external pressures [1]. Veins serve as essential blood reservoirs, accounting for approximately 70% of total blood volume [2]. Intravenous fluids are the most commonly used drugs in hospitalized patients [3]. An accurate assessment of blood volume status, predominantly reflected in the venous system, plays a crucial role in the planning of patient treatment across various medical disciplines, including cardiology, emergency medicine, internal medicine, and general practice [4].

The inferior vena cava (IVC), the largest vein in the human body, traverses the abdominal cavity and penetrates the thoracic diaphragm at the caval opening, ultimately connecting to the right atrium. The dimensions and collapsibility of the IVC are correlated with critical clinical parameters, including the right atrial pressure (RAP) [5,6], the fluid distribution within the venous compartment, and the overall volume status of patients [1,7,8]. Ultrasound (US) scans offer a promising avenue for IVC assessment. This non-invasive, cost-effective technique provides rapid results without adverse effects [9]. Notably, IVC US guidance is beneficial for managing patients with hypotension [10]. Moreover, the analysis of the IVC's diameter can be used to evaluate essential parameters (e.g., mortality risks), but also for illness identification (e.g., septic shock or congestive heart failure) [10]. Its investigation via US scans allows to measure respirophasic variations of IVC's diameter, quantified in terms of the caval index (CI), which is defined as the relative variation during the respiratory cycle with respect to its maximal value [11]:

$$CI = \frac{max(D) - min(D)}{max(D)} \tag{1}$$

However, this method raises many concerns about standardization, operator dependence, and measurement errors [12–14]. Specifically, movements of the IVC [11] and non-uniform collapsibility [15,16] challenge the investigation along a single direction, i.e., using M-mode visualization. Therefore, even when considering the strong need for a non-invasive monitoring method in clinics [17], poor accuracy is still observed when IVC indexes are used in applications, e.g., to estimate volume responsiveness [18] and right atrial pressure [19]. Different methods have been proposed to compensate some movements [20] and to process two-dimensional (2D) IVC sections from B-mode US scans [15,16,21–23]. However, it is expected that advanced methods based on 2D processing of IVC sections in long [15,21,22] or short axes [16,23] could have problems in managing the three-dimensional in an orthogonal orientation to the tilt plane [24].

In fact, B-mode US scans provide information on the IVC geometry in a single plane. A phantom of an IVC with a conic shape is represented in Figure 1. Specifically, the sections in two perpendicular planes are shown in Figure 1A, and the three-dimensional IVC model is provided in Figure 1B. Furthermore, Figure 1C provides two example frames, one in the long axis and the other in the short axis, which illustrate how the phantom IVC might appear in an actual US scan. Referring again to Figure 1A, the intersection between the IVC and the tilt plane changes when respirophasic movements induce translations in cranio-caudal and medio-lateral directions [11]. The first affects the cross-section visualized in the short-axis view, whereas the latter influences the long-axis section. Moreover, small rotations of the IVC with respect to the US probe are expected, as the transducer is following abdominal movements during the recording. Referring to Figure 1B, the pitch (i.e., an in-plane rotation of the IVC) can be compensated in the long-axis view, if a 2D processing is used. On the other hand, the short-axis view is directly affected by such a rotation: for example, if the IVC is a perfect cylinder with a circular section, the cross-section is circular only if the vector orthogonal to the tilt plane is parallel to the axis of the cylinder, otherwise it is an ellipse, with area increasing with the pitch. The roll (i.e., a rotation of the IVC around its axis) does not affect the transverse view (as the entire cross-section is visualized), but it influences the long-axis view, except in the case in which the cross-section is a perfect circle. The yaw (i.e., a rotation of the IVC around a vertical axis) would make the IVC be out of plane, generating a variation of the visualized sections in both long- and short-axis views.
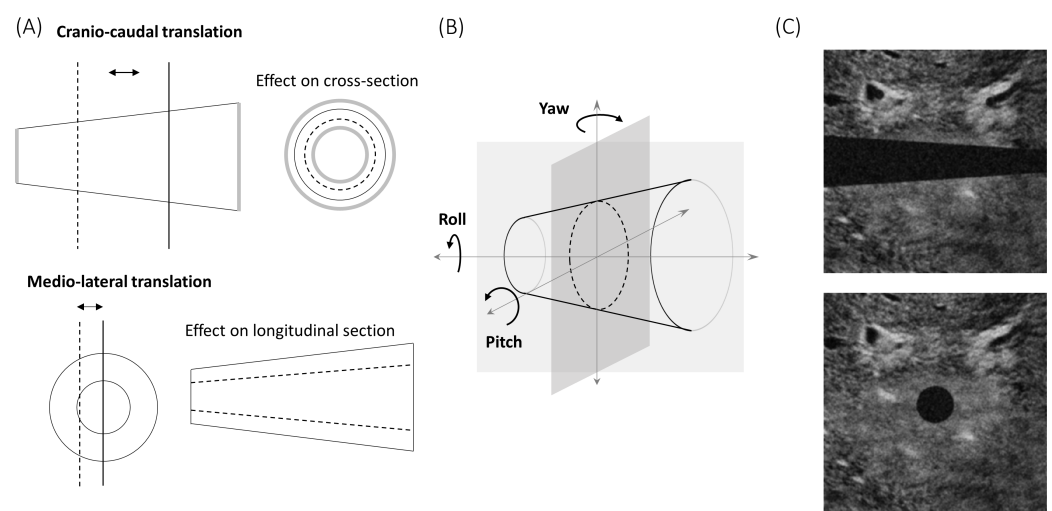
Figure 1. (**A**) Possible translations of the inferior vena cava (IVC) with respect to the tilt plane. (**B**) Possible rotations of the IVC with respect to the tilt plane. (**C**) Example of simulated frames in long- and short-axis views.

In this paper, the limitations of analyzing a vessel with single 2D views (long and short axes) are documented, and a novel method to integrate their information is proposed. The long- and short-axis views are assumed to be conveniently acquired synchronously, with an US

system with an X-plane visualization. Then, the proposed method provides an approximate estimation of the volume of the IVC (using the long- and short-axis views), from which a global 1D measurement of size (i.e., an equivalent diameter) is obtained. The algorithm to integrate the two views is explained in the Methods section, together with the description of a simulator designed to validate the method's functionality in different conditions. The simulator is designed to represent reasonable relative movements between the tilt plane of an US probe and a blood vessel like the IVC. The equivalent diameters estimated by 2D edge tracking (from long- and short-axis views) and the new algorithm can be compared. The outcomes of our study are detailed in the Results section. A preliminary experimental test is also shown. A more detailed experimental application of our method is discussed in our recent paper [25]. Then, in the Discussion section, we examine the limitations associated with long- and short-axis views of the IVC. Furthermore, we analyze the supplementary information obtained synchronously from an US system equipped with an X-plane visualization and the benefit derived from our algorithm. Finally, limitations and future works are also detailed.

2. Methods

An algorithm (implemented in Matlab, 2024a the Mathworks) was developed to integrate the outputs of two edge tracking algorithms, processing US scans of IVC either in long- [15] or in short-axis views [16]. The method (described below) was then tested on simulated videos, representing translations and rotations of the IVC.

2.1. Algorithm

The long- and short-axis views can be measured synchronously by an US system in an X-plane. They were simulated and then used to estimate the volume of a small portion of the IVC, from which an average diameter was computed as a measure of its size. The two views provide, for each frame, the section of the IVC in two orthogonal planes. This is a limited component of the IVC's geometry. Thus, we made an approximate estimation of the volume of a portion of the IVC, based on the following hypotheses.

H1. The portion of the IVC has a cross-section with same shape along the longitudinal direction.

H2. The axis of the IVC (i.e., the geometric locus of the centroids of the cross-sections) is on a plane parallel to the long-axis section (see Figure 2).
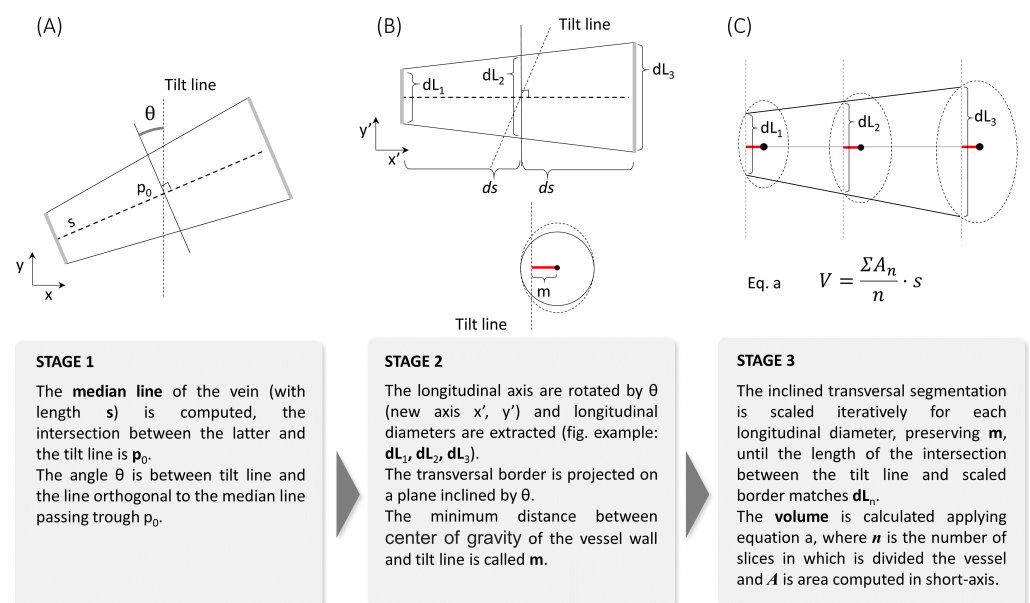

$$V = \frac{\Sigma A_n}{n} \cdot s$$

STAGE 1

The **median line** of the vein (with length **s**) is computed, the intersection between the latter and the tilt line is p_0.
The angle θ is between tilt line and the line orthogonal to the median line passing trough p_0.

STAGE 2

The longitudinal axis are rotated by θ (new axis x', y') and longitudinal diameters are extracted (fig. example: dL_1, dL_2, dL_3).
The transversal border is projected on a plane inclined by θ.
The minimum distance between center of gravity of the vessel wall and tilt line is called **m**.

STAGE 3

The inclined transversal segmentation is scaled iteratively for each longitudinal diameter, preserving **m**, until the length of the intersection between the tilt line and scaled border matches dL_n.
The **volume** is calculated applying equation a, where **n** is the number of slices in which is divided the vessel and *A* is area computed in short-axis.

Figure 2. Illustration of the method used to estimate the volume of a portion of the IVC from long- and short-axis views. The three steps are shown and explained in (**A**), (**B**), and (**C**), respectively.

Notice that, in a general IVC, the cross-section can change shape in time, as monitored by the short-axis view. Shape variations are due both to the displacements of the IVC and to the size variations induced by changes in transmural pressure. Exploring the longitudinal view, the translations of the IVC can be estimated, but the concomitant pressure variations are unknown; thus, the information on IVC's shape out of the visualized sections is not completely available. Thus, the first hypothesis H1 (even if arbitrary) is needed to fix this lack of information. It can be only approximately true, as it is expected that the shape of the cross-section of IVC can change with the location, e.g., due to the presence of tissues leaning against or anchoring the vessel. However, by wisely selecting a small portion of the vein, the approximation is expected to be reasonably good.

The second hypothesis H2 fixes another indeterminacy. In fact, an infinite number of vessels could have the same intersections with the two orthogonal tilt planes on which long- and short-axis views are taken. Indeed, different complicated geometries could be thought if we imagine a vessel with a curvilinear axis and cross-sections that adapt their dimension (and possibly also their shape, if neither the first hypothesis holds) so that the long-axis view is matched. Thus, a constraint is needed again. Our hypothesis assumes that the distance from the barycenter of each cross-section and the longitudinal plane is constant. Again, this could be considered valid within a reasonable approximation under the hypotheses that the operator is careful to measure a section parallel to the longitudinal course of the vein and that the IVC does not bend (and therefore it has an almost straight axis). Again, this condition could be met more easily if the considered portion of the IVC is small.

Under the above-mentioned hypotheses, the volume of the portion of IVC can be computed as follows (see Figures 2 and 3).

1. From the longitudinal view, IVC's midline is computed as the mean of the two estimated edges.
2. The edges estimated in the transverse view are projected on a plane passing through the point p_0 of the intersection of the short-axis section with the midline while being orthogonal to it.
3. The volume integral is computed as the sum of layers, parallel to the projected cross-section computed on the previous step and all with the same shape (following the first hypothesis H1). These layers are scaled in order that their intersections with the longitudinal plane match the long-axis view. Optimal scaling is computed by the interior point algorithm, imposing the following requirements: matching of the diameter D found on the longitudinal section; maximal scale variation of 10% with respect to D/D_0, where D_0 is the diameter in direction orthogonal to the midline and in the plane through p_0; and fixed distance L from the axis (following the second hypothesis H2).

These steps are explained in Figure 2, where specific projections on long- and short-axis views are assumed for a prototype of a vessel. Figure 3 shows a flow chart of the method, using the same pictures as in Figure 2 as the reference.

Notice that the cranio-caudal movements of the IVC are tracked in the longitudinal view, but the transverse cross-section is fixed. Thus, the longitudinal range of integration changes according to IVC's movements. In order to better fit the hypotheses of our interpretation model, it is advisable that the transverse section is around the mean location of the portion of the IVC that is integrated, which oscillates with the respiratory cycles, allowing the average central cross-section of the volume portion being monitored by the short-axis view.

Once the volume of the portion of the IVC of interest is calculated, a 1D size measurement, i.e., an equivalent diameter, is determined, in order to be comparable with estimates obtained using either the longitudinal or the transverse section, from which average diameters are also derived. Specifically, an equivalent diameter is computed for each estimated cross-section using the formula

$$D_i = 2\sqrt{\frac{A_i}{\pi}} \tag{2}$$

where the subscript i indicates the ith cross-section, with A_i being its area. Then, the estimates are averaged

$$D = \frac{\sum\limits_{i=1}^{N} D_i}{N} \tag{3}$$

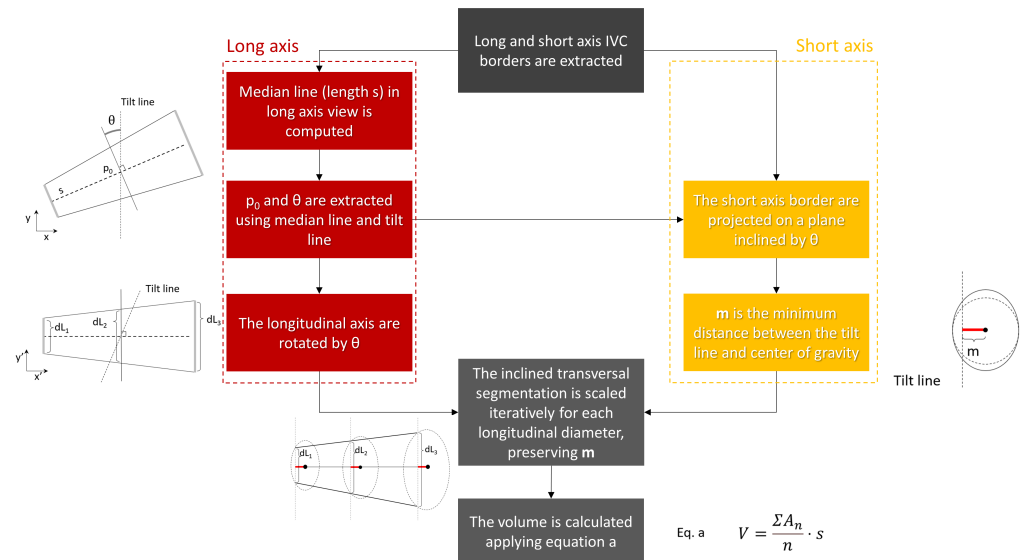where N is the number of cross-sections considered.

Figure 3. Flow chart of the proposed method to integrate information from long- [15] and short-axis [16] views obtained by two edge tracking algorithms.

2.2. Simulations

The estimations of the new algorithm were compared to those obtained from the 2D views (longitudinal and transverse), when applied on simulated frames. The algorithm was developed in Matlab. A rigid IVC in the shape of a truncated cone was simulated, either translating or rotating with respect to the two orthogonal tilt planes, providing long- and short-axis views, respectively. Once we found the intersections of the cone with the two planes, a simulated echographic frame was built, as follows. At the exterior of the cone, a portion of a real frame showing tissues around the IVC was placed. The lumen of the IVC was dark. Then, additive Gaussian and speckle noises were added, with different energies, in order to test the stability of the estimations when processing noisy data. Figure 1C shows an example of a frame in long- and short-axis views.

For each considered simulation, the generated frames were used to build two videos as an output, showing the long- and the short-axis views, respectively. Then, each simulated video was analyzed by the segmentation algorithms for edge tracking in long [15] and short axes [16]. Finally, the new algorithm integrated this information, providing an estimate of the equivalent diameter to be compared with that obtained from each of the 2D views.

3. Results

Figures 4–7 show the estimation of the equivalent diameter obtained considering either the 2D approaches (long- and short-axis views) or the new one. The methods were applied to simulated frames, showing a rigid IVC with the shape of a cone, making different movements. Thus, the correct diameter to be estimated was a constant value (100 pixels for Figures 4–6 and 105.8 pixels for Figure 7).

Figure 4 considers translations along the longitudinal directions. The location of the IVC is making an oscillation, moving first toward the left and then on the right of the initial position. The transverse section is largely affected by the displacement, which is orthogonal

to the directions which are visualized, whereas the long-axis view is unaffected, as the tracking compensates movements in the longitudinal plane.
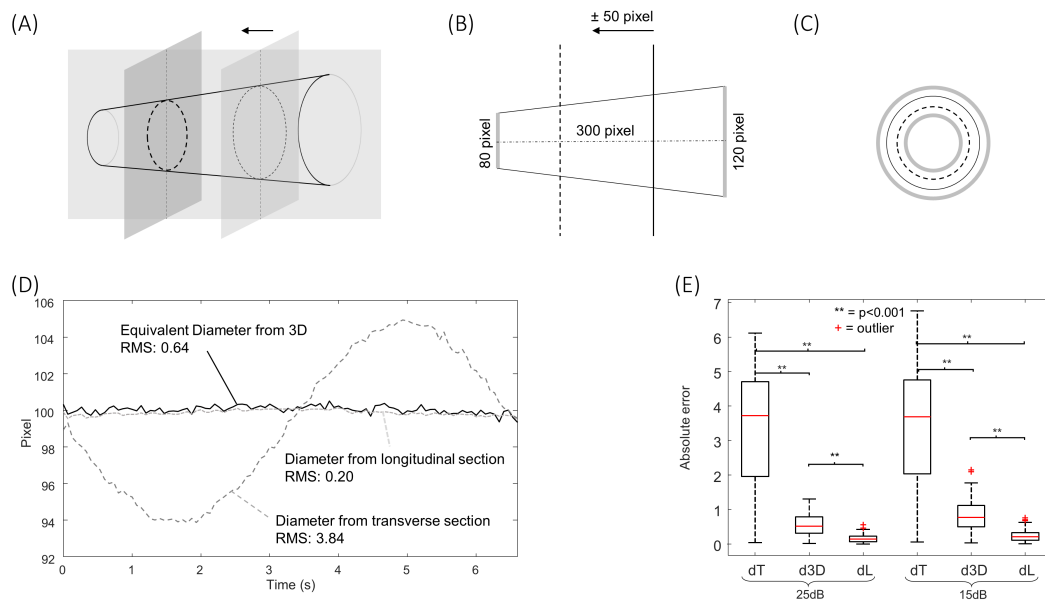

Figure 4. Effect of translations along the longitudinal directions on the equivalent diameter estimated by three methods, based on 2D longitudinal and transverse views, or the 3D approach. The location of the IVC is making an oscillation, moving first toward the left and then to the right of the initial position. (**A**) Representation of the movement in 3D. (**B**) Illustration of the long-axis view. (**C**) Cross-section. (**D**) Estimations of IVC diameter obtained considering SNR of 25 dB (the correct diameter is 100 pixels). The root mean squared errors are indicated in the figure. (**E**) Absolute error of diameter estimation by the transverse view (dT), the new approach (d3D), and the long-axis section (dL), considering noise with different power. Statistical differences under the Wilcoxon signed rank test are indicated ($p < 0.001$).
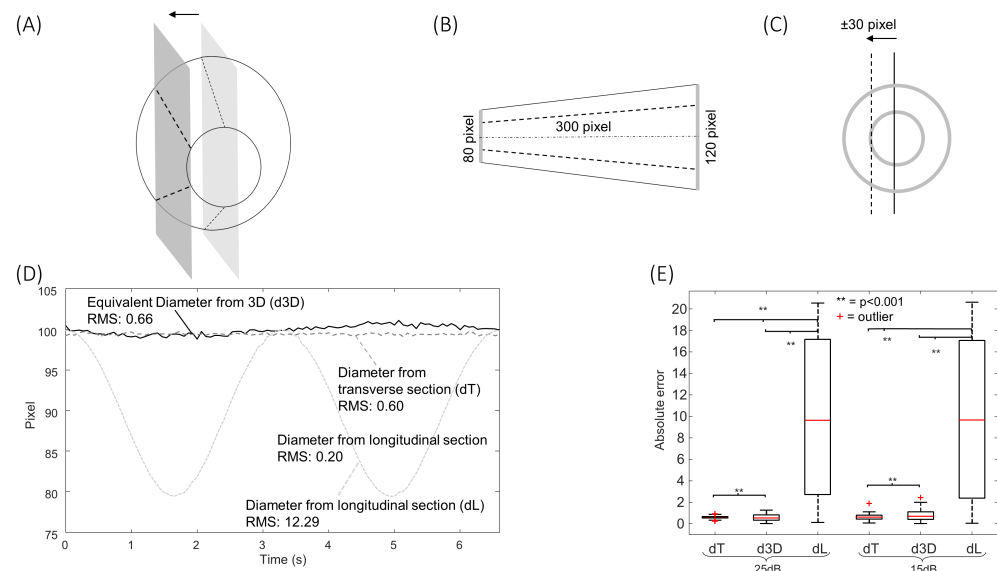

Figure 5. Same format as Figure 4, but considering translations along the medio-lateral direction.

Figure 5 shows the effect of translations along the medio-lateral direction. As for Figure 4, a cycle of an oscillation is considered. In this case, the diameter estimation in the long-axis view is largely affected, whereas the cross-section could be correctly tracked in the transverse plane.
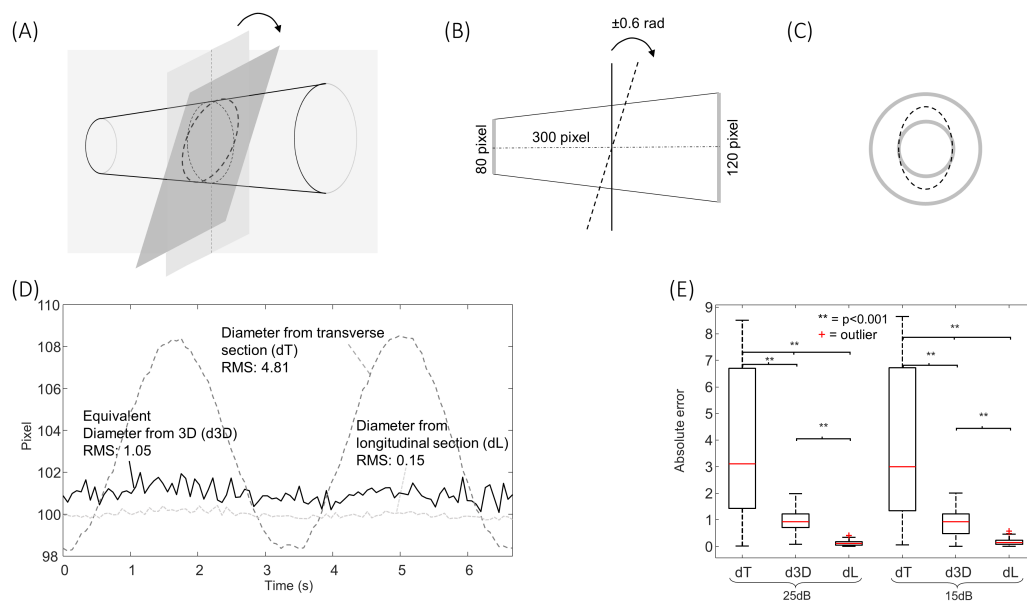
Figure 6. Same format as Figure 4, but considering oscillations of the value of pitch, varying between about ±34.4°.

Figure 6 shows the effect of an oscillation of the value of the pitch (with a maximal rotation angle of 18°). The algorithm processing the longitudinal section is able to compensate for this rotation (as it develops within the long axis plane). On the other hand, the short-axis view is affected.
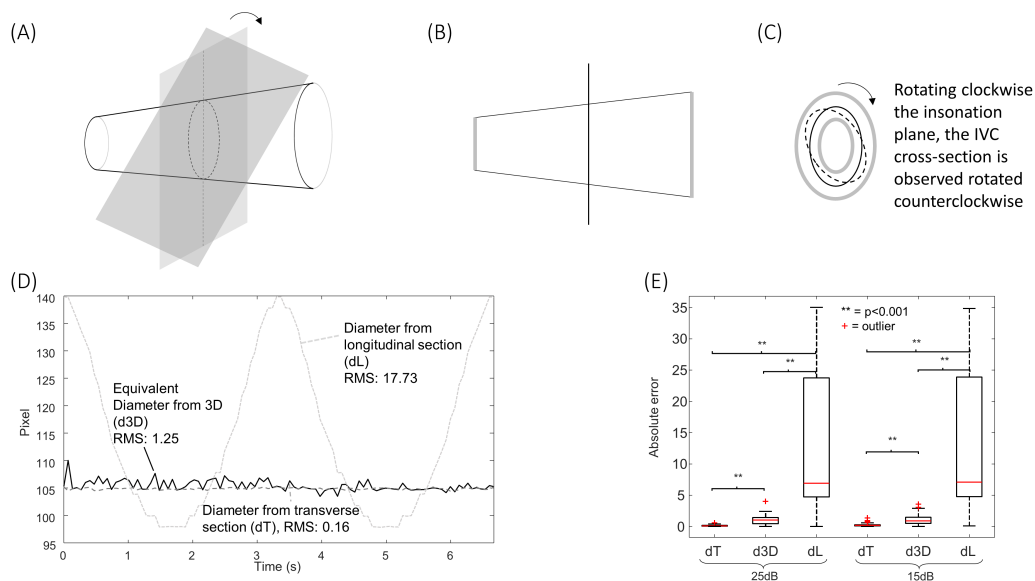

Figure 7. Same format as Figure 4, but considering oscillations of the value of roll varying between ±45° and a vein with ellipsoidal cross-section, with semiaxes in the central section (visualized by the short view) of 40 and 70 pixels; thus, the correct equivalent diameter is 105.8 pixels.

In all cases, the new algorithm was able to compensate for the simulated movements. The estimation errors were larger when increasing the noise level, as expected. The extent of the problem depends on the extension of the movement and on the shape of the IVC.

Other movements are possible. For example, the roll would not affect the estimations for the cone-shaped IVC considered in Figures 4–6, as the cross-section is circular, but it would change the long-axis view if the cross-section had any other arbitrary shape. As

an example, Figure 7 shows the case of a simulated IVC with an ellipsoidal cross-section while it is rolling.

Moreover, the yaw would affect the estimations, as the IVC would be out of plane and there is no way to understand it from the two views.

In practice, a combination of different movements of the IVC is expected in experimental recordings. They cannot be inspected in detail by two sequential acquisitions in B-mode in long and short axes (which could be aligned by synchronizing them with respect to the respiration and heart cycles). Indeed, the additional information of the relative position of the two scanning planes would not be available in that case, but it is fundamental. Figure 8 provides a sketched representation of this situation, considering a pair of frames of experimental data in B-mode. They show the IVC in long and short axes, respectively. As it is not possible to precisely control the relative locations of the scanned planes in B-mode, we assumed that the recorded frames resulted from two different sections, related by a longitudinal displacement of the cross-section (as in Figure 4) together with a medio-lateral shift of the longitudinal section (as in Figure 5) to obtain compatible configurations. Two very different IVC geometries are required to justify the two recorded frames in those conditions. Accordingly, different volumes and equivalent diameters would be needed to correctly characterize the vein, which are not available with neither single nor sequential B-mode acquisitions. Notice that Figure 8 shows only two examples of configurations, but the considered two frames could were taken from IVCs with other geometries: for example, the cross-section could have been acquired with a pitch angle with respect to the IVC axis (investigated in Figure 6), providing a bias in estimating the equivalent diameter, which would be larger than that of the true cross-section of the studied portion.
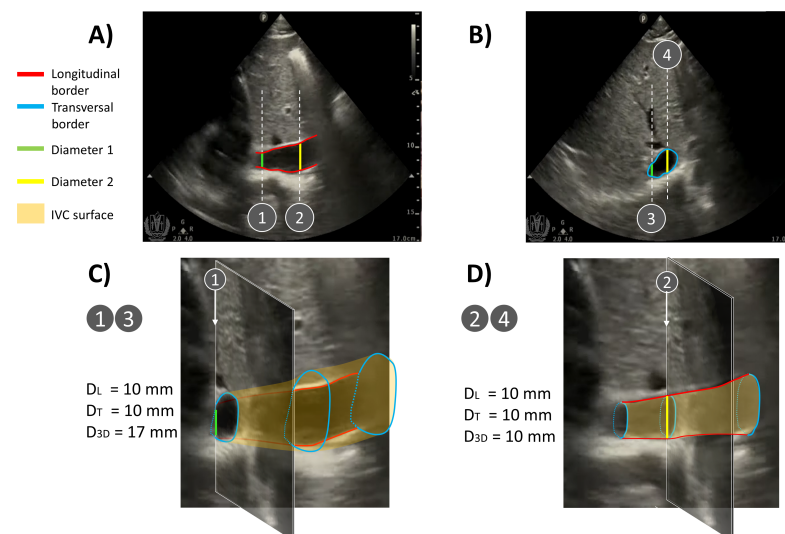

Figure 8. Representative example of two different IVC geometries compatible with the same two B-mode acquisitions in (**A**) long and (**B**) short axes, respectively (frames extracted from [26]). The two frames are assumed to be taken in the same conditions (i.e., ideally in the same time sample or at the same point along the respiratory and heartbeat cycles), but without knowing the direction of each scanning plane (available only in X-plane mode). Very different IVC geometries can be deduced, depending on the relative positions of the scanning planes, obtaining different estimations of equivalent diameters (D_L, D_T, and D_{3D}, which are the estimated equivalent diameters from the longitudinal, transversal, and X-plane views, respectively). (**C**) If the long-axis plane is displaced in the medio-lateral direction with respect to the center of the IVC, the two frames are compatible with an IVC with a large volume (notice that the green segment has the same length in the frames shown in the top panel). (**D**) If the long-axis section is on the IVC axis, the volume of the vein is much smaller than in the previous case (notice that the yellow segment has the same length in the frames shown in the top panel).

These observations were recently confirmed using experimental data from eight healthy subjects recorded by a US system in an X-plane configuration, where we documented the problems induced by movements of the IVC outside the section displayed in B-mode scans (either in long or short axes) [25]. We compared the proposed estimation of IVC's diameter with those obtained using 2D US scans. The following problems were observed: median error of 17% using a long-axis view of the IVC was affected by medio-lateral displacements (median of 4 mm); 7% and 9% of median error when measuring the IVC diameter from a short-axis view in the presence of pitch angle (median of 0.12 radians) and cranio-caudal movement (median of 15 mm), respectively.

4. Discussion

This paper introduces an innovative method to estimate size changes of blood vessels from synchronous US scans acquired from two orthogonal tilt planes, providing long- and short-axis views. The algorithm is supposed to be applied on the inferior vena cava (IVC), which is a large and deep blood vessel that undergoes important movements and deformations.

4.1. The Need of Investigating the IVC in 3D

The geometry of the IVC can be very complicated and vary in different patients: its section can vary a lot along a direction longitudinal to the axis [15,20], and the cross-section can be very different [16], as a function of the specific anatomy and the level of filling (which also changes during respiration). For these reasons, exploring IVC's edges in an entire section provides a more reliable characterization than along a single direction [15,16], as performed in clinical practice.

However, even an entire section can be affected by IVC's movements, which can affect measurements: for example, off-midline displacement results in a smaller measurement of IVC's size in the longitudinal view [11], and a roll makes exploring a different section more difficult (which is different if the cross-section is not a perfect circle); movements in the cephalic or caudal direction affect the short-axis view as it is taken at different anatomic sections [11], and a relative rotation pitch between the IVC and probe increases the measured cross-section (which is minimal when the tilt plane is orthogonal to the IVC axis).

The only solution would be exploring the IVC in 3D [27]. However, taking a full 3D IVC scan could take a long time or would provide images with a low resolution, impeding the study of its collapsibility. As an approximation, long- and short-axis views can be acquired synchronously with an US system in X-plane mode. In this way, the two sections are acquired at the same time and information from the two views can be integrated. Moreover, the two sections can have a good spatial resolution and a sampling frequency still sufficient to follow IVC dynamics (for example, in our recent study [25], the frame rates dropped from about 60 Hz in B-mode to 30 Hz in the X-plane, which is still sufficient to investigate IVC's collapsibility). Here, we propose to make an approximate estimation of the volume of a portion of the IVC. The vessel is tracked in order to compensate movements in the cranio-caudal and medio-lateral directions. Moreover, the cross-section is projected in the direction orthogonal to the midline. In this way, the aforementioned limits of the two views are overcome.

The method is validated using simulations as the gold standard. The estimations are stable regarding cranio-caudal movements (Figure 4), medio-lateral movements (Figure 5), pitch rotations (Figure 6), and rolls (Figure 7), whereas the method cannot compensate for a yaw rotation (i.e., the IVC is out of plane) or complicated geometries of the vein (e.g., bending or cross-sections along the longitudinal course which are much different from linear scaling of the recorded short-axis view). A comparison of the equivalent IVC diameters estimated by the proposed method and using single B-mode scans has been recently investigated with experimental data, showing relevant effects of IVC movements out of visualized planes [25].

4.2. Limitations

The proposed method effectively compensates for some problems that B-mode visualization-based techniques cannot address. However, it has some limitations that must be acknowledged. It makes some assumptions on tilt planes and on the shape of the IVC in order to estimate its volume. In fact, the shape of the IVC out of the two tilt planes is not known, and infinite geometries could perfectly fit the recorded scans. Specifically, we assumed that the IVC is straight and aligned to the long-axis plane; moreover, we supposed that the cross-section has the same shape and changes only the dimension along the course of the blood vessel. We could say that we are making a first-order approximation that can hold as long as the portion of the investigated IVC is small. The extension of the IVC portion guaranteeing that the approximation is feasible should depend on the size of the vessel, e.g., we advise not to go beyond 2–3 times the IVC's diameter. Beyond this limit, we expect that it is difficult to fit the hypotheses that the IVC is straight, the shape is constant, and the long-axis section is aligned to the midline.

A further limitation is the need of using an advanced echography system, with a 2D probe allowing for X-plane acquisition. Using separate long- and short-axis views and then synchronizing them (e.g., considering short acquisitions in breath holding and synchronizing with respect to the heartbeat) would not provide complete information, as the location and orientation of each tilt plane is available only when using the X-plane.

Another marginal problem is that the frame rate is two times lower when performing acquisition in the X-plane than in B-mode. However, the sampling rate is usually still sufficient to recover information on IVC's size and collapsibility, which are of primary interest.

Finally, we should consider that optimizing the estimation of IVC's diameter is only a specific detail useful for accurately defining the volume status of a patient. In fact, many other confounding factors should be addressed to achieve a stable and accurate evaluation of the patient. Indeed, the variation in IVC's diameter depends on transmural pressure, which is defined on the basis of two unknowns: the pressures outside and inside the IVC. Moreover, the modality of respiration of the patient directly affects IVC's dynamics [28]. Therefore, estimating the size of the IVC, even if accurate, is not sufficient, and it needs to be corroborated by further efforts to standardize the clinical investigation [1].

4.3. Future Perspectives

The use of US videos in the X-plane allows us to compensate for possible problems due to translations or rotations of the IVC relative to the probe. These movements are expected to be in phase with respiration, so that their effect is superimposed to IVC's respirophasic collapsibility. Thus, being able to compensate for them can improve the reliability of the assessment of IVC's size and collapsibility. This could have immediate clinical outcomes. In fact, the non-invasive monitoring of IVC's size and its collapsibility using US scans may find many applications [1], such as in the assessment of a patient's volemic status, estimation of right atrial pressure, assessment of venous compliance and fluid redistribution, monitoring responses during renal dialysis, to diuretics, or a fluid challenge. Moreover, the same approach can be applied to track arterial phasic deformations [29], allowing us to have the possibility of evaluating the arterial stiffness and assessing cardiovascular health.

These important applications can be addressed by acquiring US scans with the same techniques already used in clinics, but using an advanced system providing X-plane visualization and applying the proposed algorithm to assess IVC's diameter. However, even more stable indications could be obtained by refining the measurement technique used here. In fact, our long-standing work is devoted to defining a measurement protocol and solving technical problems in the processing of US scans of the IVC in order to obtain more reliable information than that currently recorded in the clinic. In the present work, we have only considered one specific piece of the puzzle (i.e., the attempt to optimize the estimation of IVC's diameter), but there is still a long way to go. Once we can accurately estimate IVC's diameter over time, it will be possible to divide the cardiac and respiratory components [1], which could possibly provide selective information on cardiac and pulmonary contributions

(still to be accurately investigated). However, we should consider that the modality of respiration could be an important confounding factor [28]: thus, an important future work is to standardize the respiration cycles performed by the patient in order to make the information provided by IVC's collapsibility indexes more reliable.

Moreover, many future works are needed to assess the performances of our algorithm in real scenarios, for example, the repeatability of the estimations in physiology (i.e., making tests on healthy subjects), the assessment of patients with hydration problems (e.g., in terms of the possibility to discriminate different patients in either hypo-, eu-, or hyper-volemic conditions), and the estimation of RAP.

5. Conclusions

We introduced an algorithm to integrate the information from US videos in long- and short-axis views recorded by a system in an X-plane configuration and to estimate the volume of a small portion of a vessel, from which its size can be computed in terms of an equivalent diameter. Different translations and rotations of the US probe with respect to blood vessels can affect the assessment of IVC's size from a single 2D view. Our algorithm was developed to compensate for longitudinal and medio-lateral translations, as well as for pitch and roll rotations. As referenced, we compared the estimations of the average size of a simulated blood vessel with different shapes and by performing various movements, when using long and short-axis views or the proposed approach. Our simulations generated US frames incorporating noise with two levels. Our tests showed that the proposed algorithm effectively compensates for vessel movements and provides a more stable estimation of blood vessels' size compared to long or short-axis views.

In prospective, this could allow us to obtain more stable information on patient hydration and central venous pressure. Future works are suggested to assess the performance of this innovative method in physiological studies and in clinical scenarios.

Author Contributions: Conceptualization, L.M.; methodology, L.M. and P.P.; software, P.P.; validation, L.M. and P.P.; data preparation, L.M.; investigation, L.M. and P.P.; writing—original draft preparation, L.M. and P.P.; writing—review and editing, L.M.; visualization, L.M. and P.P.; supervision, L.M. All authors have read and agreed to the published version of the manuscript.

Conflicts of Interest: An instrument implementing the 2D algorithms used in this paper was patented by Politecnico di Torino and Universitá di Torino (patent number WO 2018/134726) and was licensed by VIPER s.r.l.

Abbreviations

The following abbreviations are used in this manuscript:

2D	two-dimensional
3D	three-dimensional
CI	caval index
IVC	inferior vena cava
US	ultrasound

References

1. Mesin, L.; Albani, S.; Policastro, P.; Pasquero, P.; Porta, M.; Melchiorri, C.; Leonardi, G.; Albera, C.; Scacciatella, P.; Pellicori, P.; et al. Assessment of Phasic Changes of Vascular Size by Automated Edge Tracking-State of the Art and Clinical Perspectives. *Front. Cardiovasc. Med.* **2022**, *8*, 775635. [CrossRef] [PubMed]
2. Ermini, L.; Chiarello, N.E.; De Benedictis, C.; Ferraresi, C.; Roatta, S. Venous Pulse Wave Velocity variation in response to a simulated fluid challenge in healthy subjects. *Biomed. Signal Process. Control* **2021**, *63*, 102177. [CrossRef]
3. Tinawi, M. New Trends in the Utilization of Intravenous Fluids. *Cureus* **2021**, *21*, e14619. [CrossRef] [PubMed]
4. Karami, E.; Shehata, M.S.; Smith, A. Estimation and tracking of AP-diameter of the inferior vena cava in ultrasound images using a novel active circle algorithm. *Comput. Biol. Med.* **2018**, *98*, 16–25. [CrossRef] [PubMed]

5. Mesin, L.; Albani, S.; Sinagra, G. Non-invasive Estimation of Right Atrial Pressure Using Inferior Vena Cava Echography. *Ultrasound Med. Biol.* **2019**, *45*, 1331–1337. [CrossRef] [PubMed]

6. Albani, S.; Mesin, L.; Roatta, S.; De Luca, A.; Giannoni, A.; Stolfo, D.; Biava, L.; Bonino, C.; Contu, L.; Pelloni, E.; et al. Inferior Vena Cava Edge Tracking Echocardiography: A Promising Tool with Applications in Multiple Clinical Settings. *Diagnostics* **2022**, *12*, 427. [CrossRef]

7. Lichtenstein, D. Inferior vena cava. In *General Ultrasound in the Critically Ill*; Springer: Berlin, Germany, 2005; Volume 23, p. 82.

8. Mesin, L.; Roatta, S.; Pasquero, P.; Porta, M. Automated Volume Status Assessment Using Inferior Vena Cava Pulsatility. *Electronics* **2020**, *9*, 1671. [CrossRef]

9. Lentz, B.; Fong, T.; Rhyne, R.; Risko, N. A systematic review of the cost-effectiveness of ultrasound in emergency care settings. *Ultrasound J.* **2021**, *13*, 16. [CrossRef]

10. Policastro, P.; Mesin, L. Processing Ultrasound Scans of the Inferior Vena Cava: Techniques and Applications. *Bioengineering* **2023**, *10*, 1076. [CrossRef]

11. Blehar, D.; Resop, D.; Chin, B.; Dayno, M.; Gaspari, R. Inferior vena cava displacement during respirophasic ultrasound imaging. *Crit. Ultrasound J.* **2012**, *4*, 18. [CrossRef]

12. Wallace, D.; Allison, M.; Stone, M. Inferior vena cava percentage collapse during respiration is affected by the sampling location: An ultrasound study in healthy volunteers. *Acad. Emerg. Med.* **2010**, *17*, 96–99. [CrossRef] [PubMed]

13. Resnick, J.; Cydulka, R.; Platz, E.; Jones, R. Ultrasound Does Not Detect Early Blood Loss In Healthy Volunteers Donating Blood. *J. Emerg. Med.* **2011**, *41*, 270–275. [CrossRef]

14. Zhang, Z.; Xu, X.; Ye, S.; Xu, L. Ultrasonographic Measurement of the Respiratory Variation in the Inferior Vena Cava Diameter Is Predictive of Fluid Responsiveness in Critically Ill Patients: Systematic Review and Meta-analysis. *Ultrasound Med. Biol.* **2014**, *40*, 845–853. [CrossRef] [PubMed]

15. Mesin, L.; Pasquero, P.; Roatta, S. Tracking and Monitoring Pulsatility of a Portion of Inferior Vena Cava from Ultrasound Imaging in Long Axis. *Ultrasound Med. Biol.* **2019**, *45*, 1338–1343. [CrossRef]

16. Mesin, L.; Pasquero, P.; Roatta, S. Multi-directional assessment of Respiratory and Cardiac Pulsatility of the Inferior Vena Cava from Ultrasound Imaging in Short Axis. *Ultrasound Med Biol.* **2020**, *46*, 3475–3482. [CrossRef]

17. Millington, S. Ultrasound assessment of the inferior vena cava for fluid responsiveness: Easy, fun, but unlikely to be helpful. *Can. J. Anaesth.* **2019**, *66*, 633–638. [CrossRef]

18. Orso, D.; Paoli, I.; Piani, T.; Cilenti, F.L.; Cristiani, L.; Guglielmo, N. Accuracy of Ultrasonographic Measurements of Inferior Vena Cava to Determine Fluid Responsiveness: A Systematic Review and Meta-Analysis. *J. Intensive Care Med.* **2020**, *35*, 354–363. [CrossRef] [PubMed]

19. Magnino, C.; Omede, P.; Avenatti, E.; Presutti, D.G.; Iannaccone, A.; Chiarlo, M.; Moretti, C.; Gaita, F.; Veglio, F.; Milan, A. Inaccuracy of Right Atrial Pressure Estimates Through Inferior Vena Cava Indices. *Am. J. Cardiol.* **2017**, *120*, 1667–1673. [CrossRef]

20. Mesin, L.; Pasquero, P.; Albani, S.; Porta, M.; Roatta, S. Semi-automated tracking and continuous monitoring of inferior vena cava diameter in simulated and experimental ultrasound imaging. *Ultrasound Med. Biol.* **2015**, *41*, 845–857. [CrossRef]

21. Sonoo, T.; Nakamura, K.; Ando, T.; Sen, K.; Maeda, A.; Kobayashi, E.; Sakuma, I.; Doi, K.; Nakajima, S.; Yahagi, N. Prospective analysis of cardiac collapsibility of inferior vena cava using ultrasonography. *J. Crit. Care* **2015**, *30*, 945–948. [CrossRef]

22. Mesin, L.; Giovinazzo, T.; D'Alessandro, S.; Roatta, S.; Raviolo, A.; Chiacchiarini, F.; Porta, M.; Pasquero, P. Improved repeatability of the estimation of pulsatility of inferior vena cava. *Ultrasound Med. Biol.* **2019**, *45*, 2830–2843. [CrossRef]

23. Nakamura, K.; Tomida, M.; Ando, T.; Sen, K.; Inokuchi, R.; Kobayashi, E.; Nakajima, S.; Sakuma, I.; Yahagi, N. Cardiac variation of inferior vena cava: New concept in the evaluation of intravascular blood volume. *J. Med. Ultrason.* **2013**, *40*, 205–209. [CrossRef]

24. Huguet, R.; Fard, D.; d'Humieres, T.; Brault-Meslin, O.; Faivre, L.; Nahory, L.; Dubois-Randé, J.; Ternacle, J.; Oliver, L.; Lim, P. Three-Dimensional Inferior Vena Cava for Assessing Central Venous Pressure in Patients with Cardiogenic Shock. *J. Am. Soc. Echocardiogr.* **2018**, *31*, 1034–1043. [CrossRef] [PubMed]

25. Policastro, P.; Ermini, L.; Civera, S.; Albani, S.; Musumeci, G.; Roatta, S.; Mesin, L. Effects of respirophasic displacements of inferior vena cava on size measurements from two dimensional ultrasound imaging. *Ultrasound Med. Biol.* **2024**.

26. Pocus 101, IVC Ultrasound STEP by STEP-Easiest Method. 2015. Available online: https://www.youtube.com/watch?v=vmmrjy1bhEc (accessed on 16 June 2024).

27. Huang, Q.; Zeng, Z. A Review on Real-Time 3D Ultrasound Imaging Technology. *Biomed Res. Int.* **2017**, *2017*, 6027029. [CrossRef] [PubMed]

28. Folino, A.; Benzo, M.; Pasquero, P.; Laguzzi, A.; Mesin, L.; Messere, A.; Porta, M. Roatta, S. Vena cava responsiveness to controlled isovolumetric respiratory efforts. *J. Ultrasound Med.* **2017**, *36*, 2113–2123. [CrossRef] [PubMed]

29. Mesin, L.; Floris, L.; Policastro, P.; Albani, S.; Scacciatella, P.; Pugliese, N.; Masi, S.; Grillo, A.; Fabris, B.; Antonini-Canterin, F. Estimation of Aortic Stiffness with Bramwell–Hill Equation: A Comparative Analysis with Carotid–Femoral Pulse Wave Velocity. *Bioengineering* **2022**, *9*, 265. [CrossRef]